Shape Reconstruction from Cast Shadows using Coplanarities and Metric Constraints

Hiroshi Kawasaki[1] and Ryo Furukawa[2]

[1] Faculty of Engineering, Saitama University,
255, Shimo-okubo, Sakura-ku, Saitama, Japan
kawasaki@cgv.ics.saitama-u.ac.jp
[2] Faculty of Information Sciences, Hiroshima City University,
3-4-1, Ozuka-higashi, Asaminami-ku, Hiroshima, Japan
ryo-f@cs.hiroshima-cu.ac.jp

Abstract. To date, various techniques of shape reconstruction using cast shadows have been proposed. The techniques have the advantage that they can be applied to various scenes including outdoor scenes without using special devices. Previously proposed techniques usually require calibration of camera parameters and light source positions, and such calibration processes make the application ranges limited. If a shape can be reconstructed even when these values are unknown, the technique can be used to wider range of applications. In this paper, we propose a method to realize such a technique by constructing simultaneous equations from coplanarities and metric constraints , which are observed by cast shadows of straight edges and visible planes in the scenes, and solving them. We conducted experiments using simulated and real images to verify the technique.

1 Introduction

To date, various techniques of scene shape reconstruction using shadows have been proposed. One of the advantages of using shadows is that the information for 3D reconstruction can be acquired without using special devices, since shadows exist wherever light is present. For example, these techniques are applicable to outdoor poles on a sunny day or indoor objects under a room light. Another advantage of shape reconstruction using shadows is that only a single camera is required.

So far, most previously proposed methods assumed known light source positions because, if they are unknown, there are ambiguities on the solution and Euclidean reconstruction can not be achieved[1]. If a shape can be reconstructed with unknown light source positions, the technique can be used to wider applications. For example, a scene captured by a remote web camera under unknown lighting environments could be reconstructed. Since intrinsic parameters of a remote camera are usually unknown, if the focal length of the camera can be estimated at the same time, the application becomes more useful. In this paper, we propose a method to achieve this. Our technique is actually more general, *i.e.* both the object that casts shadows and the light source can be freely moved while scanning because both of their positions are not required to be known and static. This is a great advantage for actual scanning processes, since the unmeasured area caused by self-shadows can be drastically reduced by moving the light source.

To actually realize the technique, we propose a novel formulation of simultaneous linear equations from planes created by shadows of straight edges (shadow planes) and the real planes in the scene , which are extension of the previous studies for shape from planes [**?**,**?**] and interpretation of line drawings of polyhedrons [2]. Since shadow planes and the real planes are treated equally in our formulation, various geometrical constraints among the planes can be utilized efficiently for Euclidean upgrade and camera calibration.

In this paper, we assume two typical situations to reconstruct the scene. The first one, which we call *"shadows of the static object"*, assumes a fixed camera position, a static scene, and a static object of a straight edge which casts a moving shadow as the light source(*e.g.* the sun or a point light) moves. The second one, which we call *"active scan by cast shadow"*, assumes a fixed camera, and arbitrary motion of both a light source and an object with a straight edge to generate shadows to conduct an active scan.

2 Related work

3D reconstruction using information of shadows has a long history. Shafer *et al.* presented the mathematical formulation of shadow geometries and derived constraints for surface orientation from shadow boundaries [3]. Hambrick *et al.* proposed a method for classifying boundaries of shadow regions [4]. Several methods for recovering 3D shapes up to Euclidean reconstruction based on geometrical constraints of cast-shadows have been proposed [5,6,7,8]. All of these methods assumes that the object that casts shadows are static and the light directions or positions are known.

On the other hand, Bouguet *et al.* proposed a method which allowed users to move a straight edged object freely so that the shadow generated by a fixed light source sweep the object [9,10]. However, the technique requires calibration of camera parameters, a light source position, and a reference plane.

If an Euclidean shape can be reconstructed with unknown light source positions, it may broaden the application of "shape from cast shadow" techniques. However, it was proved that scene reconstructions based on binary shadow regions have ambiguities of four degrees of freedom (DOFs), if the light positions are unknown [1]. In the case of a perspective camera, these ambiguities correspond to the family of transformations called generalized projective bas relief (GPBR) transformations.

To deal with unknown light source positions, Caspi *et al.* proposed a method using two straight, parallel and fixed objects to cast shadows and a reference plane (*e.g.* the ground) [11]. To solve ambiguities caused by unknown light sources, they used parallelisms of shadows of straight edges by detecting vanishing points. Compared to their work, our method is more general. For example, in our method, camera can be partially calibrated, the straight object and the light source can be moved, the light source can be a parallel or point light source, and wider types of constraints than parallelisms of shadows can be used to resolve the ambiguities.

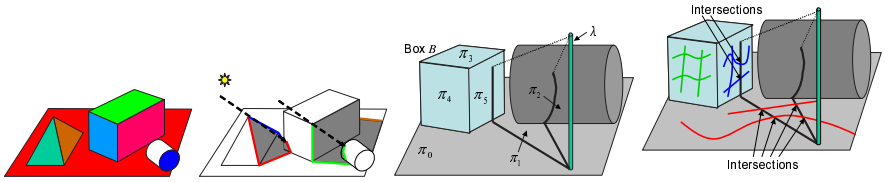

(a) (b) (c) (d)

Fig. 1. Coplanarities in a scene:(a) Explicit coplanarities. Regions of each color except for white are a set of coplanar points. Note that points on a region of a curved surface are not coplanar. (b) Implicit coplanarities. Segmented lines of each color are a set of coplanar points. (c)Examples of metric constraints: $\pi_0 \perp \pi_1$ and $\pi_0 \perp \pi_2$ if $\lambda \perp \pi_0$. $\pi_3 \perp \pi_4$, $\pi_4 \perp \pi_5$, $\pi_3 \perp \pi_5$, and $\pi_3 \parallel \pi_0$ if box B is rectangular and on π_0. (d) Intersections between explicit coplanar curves and implicit coplanar curves in a scene. Lines of each color corresponds a plane in the scene.

3 Shape Reconstruction from Cast Shadow

If a set of points exist on the same plane, they are coplanar as shown in figure 1(a). All the points on a plane are coplanar even if the plane does not have textures or feature points. A scene composed of plane structures has many coplanarities. In this paper, a coplanarity that is actually observed as a real plane in the scene is called as an *explicit coplanarity*.

As opposed to this, in a 3D space, there exist an infinite number of coplanarities that are not explicitly observed in ordinary situations, but could be observed under specific conditions. For example, a boundary of a cast-shadow of a straight edge is a set of coplanar points as shown in figure 1(b). This kind of coplanarity is not visible until the shadow is cast on the scene. In this paper, we call these coplanarities as *implicit coplanarities*. Implicit coplanarities can be observed in various situations, such as the case that buildings with straight edges are under the sun and cast shadows onto the scene. Although explicit coplanarities are observed only for limited parts of the scene, implicit coplanarities can be observed on arbitrary-shaped surfaces including free curves.

In this study, we create linear equations from the implicit coplanarities of the shadows and explicit coplanarities of the planes. By solving the acquired simultaneous equations, a scene can be reconstructed, except for four (or more) DOFs that simultaneous equations have, and also the DOFs corresponding to unknown camera parameters. For an Euclidean reconstruction from the solution, the remaining DOFs should be solved (called *metric reconstruction* in this paper). To achieve this, constraints other than coplanarities should be used. For many scenes, especially those that include artificial objects, we can find geometrical constraints among explicit and implicit planes. Examples of such information are explained here.

(1) In figure 1(c), the ground is plane π_0, and linear object λ is standing vertically on the ground. If the planes corresponding shadows of λ are π_1 and π_2, $\pi_0 \perp \pi_1$,$\pi_0 \perp \pi_2$ can be derived from $\lambda \perp \pi_0$.

(2) In the same figure, the sides of box$B$ are π_3,π_4, and π_5. If box$B$ is rectangular, π_3,π_4, and π_5 are orthogonal with each other. If box$B$ is on the ground, π_3 is parallel to π_0.

From constraints available from the scene such as above examples we can determine variables for the remaining DOFs and achieve metric reconstruction. With enough constraints, the camera parameters can be estimated at the same time. We call these constraints the *metric constraints*.

Based on this, actual flow of the algorithms are as follows.

Step 1: Extraction of coplanarities. From a series of images that are acquired from a scene with shadows captured by a fixed camera, shadow boundaries are extracted as implicit-coplanar curves. If the scene has plane areas, explicit-coplanar points are sampled from the area. For the efficient processing of steps 2 and 3 below, only selected frames are processed.

Step 2: Cast shadow reconstruction by shape from coplanarities. From a dataset of coplanarities, constraints are acquired as linear equations. By numerically solving the simultaneous equations, a space of solutions with four (or more) DOFs can be acquired.

Step 3: Metric reconstruction by metric constraints. To achieve metric reconstruction, an upgrade process of the solution of step 2 is required. The solution can be upgraded by solving the metric constraints.

Step 4: Dense shape reconstruction. The processes in steps 2 and 3 are performed on selected frames. To realize dense shape reconstruction of a scene, implicit-coplanar curves from all the images are used to reconstruct 3D shapes using the results of the preceding processes.

4 Algorithm details for each steps

4.1 Data acquisition

To detect coplanarities in a scene, the boundaries of cast shadows are required. Automatic extraction of a shadow area from a scene is not easy. However, since shadow extraction has been studied for a long period of time [12,13], many techniques are already proposed and we adopt a spatio-temporal based method as follows:

1. Images are captured from a fixed camera at fixed intervals, and a spatio-temporal image is created by stacking images after background subtraction.
2. The spatio-temporal image is divided by using 3D segmentation. The 3D segmentation has been achieved by applying a region growing method to the spatio-temporal space. To deal with noises on real images, we merge small regions to the surrounding regions and split a large region connected by a small region into two.
3. From the segmented regions, shadow regions are selected interactively by manual. Also, if wrong regions are produced by the automatic process, those regions are modified manually in this step.
4. The segmented regions are again divided into frames, and coplanar shadow curves are extracted from each frames as boundaries of divided regions.

By drawing all the detected boundaries on a single image, we can acquire many intersections. Since one intersection shares at least two planes, we can construct simultaneous equations. The numerical solution of these equations is explained in the following section.

4.2 Projective reconstruction

Suppose a set of N planes including both implicit and explicit planes. Let j-th plane of the set be π_j. We express the plane π_j by the form

$$a_j x + b_j y + c_j z + 1 = 0 \tag{1}$$

in the camera coordinates system.

Suppose a set of points such that each point of the set exists on intersections of multiple planes. Let the i-th element of the set be represented as ξ_i and exist on the intersection of π_j and π_k. Let the coordinates (u_i, v_i) be the location of the projection of ξ_i onto the image plane. We represent the camera intrinsic parameter by $\alpha = p/f$, where f is the focal length and p is the size of the pixel. We define $a_j^* = \alpha a_j$ and $b_j^* = \alpha b_j$. The direction vector of the line of sight from the camera to the point ξ_i is $(\alpha u_i, \alpha v_i, -1)$. Thus,

$$a_j(-\alpha u_i z_i) + b_j(-\alpha v_i z_i) + c_j(z_i) + 1 = 0, \tag{2}$$

where z_i is the z-coordinate of ξ_i. By dividing the form by z_i and using the substitutions of $t_i = 1/z_i$, $a_j^* = \alpha a_j$, and $b_j^* = \alpha b_j$, we get

$$-(u_i)a_j^* - (v_i)b_j^* + c_j + t_i = 0. \tag{3}$$

Since ξ_i is also on π_k,

$$-(u_i)a_k^* - (v_i)b_k^* + c_k + t_i = 0. \tag{4}$$

From the equations (3) and (4), the following simultaneous equations with variables a_j^*,b_j^* and c_j can be obtained:

$$(a_j^* - a_k^*)u_i + (b_j^* - b_k^*)v_i + (c_j - c_k) = 0. \tag{5}$$

We define $\mathbf{L}$ as the coefficient matrix of the above simultaneous equations, and $\mathbf{x}$ as the solution vector. Then, the equations can be described by a matrix form as

$$\mathbf{L}\mathbf{x} = \mathbf{0}. \tag{6}$$

Simultaneous equations of forms (5) have trivial equations that satisfy

$$a_j^* = a_k^*, b_j^* = b_k^*, c_j = c_k, (i \neq j). \tag{7}$$

Let $\mathbf{x}_1$ be the solution of $a_i^* = 1, b_i^* = 0, c_i = 0 (i = 1, 2, \ldots)$, $\mathbf{x}_2$ be the solution of $a_i^* = 0, b_i^* = 1, c_i = 0$, and $\mathbf{x}_3$ be the solution of $a_i^* = 0, b_i^* = 0, c_i = 1$. Then, the above trivial solutions form a linear space spanned by the bases of $\mathbf{x}_1$,$\mathbf{x}_2$,$\mathbf{x}_3$, which we represent as T.

We describe a numerical solution of the simultaneous equations assuming the observed coordinates (u_i, v_i) on the image plane include errors. Since the equation (6) is over-constrained, the equation generally cannot be fulfilled completely. Therefore, we consider the n-dimensional linear space S_n spanned by the n eigenvectors of $\mathbf{L}^\top\mathbf{L}$ associated with the n minimum eigenvalues. Then, S_n becomes the solution space of $\mathbf{x}$ such that $\max_{\mathbf{x}\in S_n} |\mathbf{L}\mathbf{x}|/|\mathbf{x}|$ is the minimum with respect to all possible n-dimensional linear spaces.

Even if coordinates of u_i, v_i are perturbed by additive errors, $\mathbf{x}_1$,$\mathbf{x}_2$,$\mathbf{x}_3$ remain trivial solutions that completely satisfies equations(5) within the precision of floating point calculations. Thus, normally, the 3D space S_3 becomes equivalent with the space of trivial solutions T. For non-trivial solution, we can define $\mathbf{x}_s = \mathrm{argmin}_{\mathbf{x}\in T^\perp}(|\mathbf{L}\mathbf{x}|/|\mathbf{x}|)^2$, where $T^\perp$ is the orthogonal complement space of T. $\mathbf{x}_s$ is the solution that minimizes $|\mathbf{L}\mathbf{x}|/|\mathbf{x}|$ and is orthogonal to $\mathbf{x}_1$,$\mathbf{x}_2$ and $\mathbf{x}_3$. Since T and S_3 are normally equal, $\mathbf{x}_s$ can be calculated as the eigenvector of $\mathbf{L}^\top\mathbf{L}$ associated with the 4-th minimum eigenvalue.

Thus, the general form of the non-trivial solutions are represented as

$$\mathbf{x} = f_1\mathbf{x}_1 + f_2\mathbf{x}_2 + f_3\mathbf{x}_3 + f_4\mathbf{x}_s = \mathbf{M}\mathbf{f}, \tag{8}$$

where f_1, f_2, f_3, f_4 are free variables, $\mathbf{f}$ is a vector of $(f_1\ f_2\ f_3\ f_4)^\top$, and $\mathbf{M}$ is a matrix of $(\mathbf{x}_1\ \mathbf{x}_2\ \mathbf{x}_3\ \mathbf{x}_s)$. The four DOFs of the general solution basically correspond to the DOFs of generalized projective bas-relief (GPBR) transformations described in the work of Kriegman *et al.* [1].

As far as we know, there are no previous studies that reconstruct 3D scenes by using the linear equations from the 3-DOF implicit and explicit planes. Advantages of this formulation are that the solution can be obtained stably, and the wide range of geometrical constraints can be used as metric constraints.

4.3 Metric reconstruction

The solution obtained in the previous section has four DOFs from $\mathbf{f}$. In addition, if camera parameters are unknown, additional DOFs should be resolved to achieve metric reconstruction. Since these DOFs cannot be solved using coplanarities, they should be solved using metric constraints derived from the geometrical constraints in the scene.

For example, suppose that the orthogonality between the planes π_s and π_t is assumed. We denote the unit normal vector of plane π_s as a vector function $\mathbf{n}_s(\mathbf{f},\alpha) = N((a_s(\mathbf{f},\alpha)\ b_s(\mathbf{f},\alpha)\ c_s(\mathbf{f},\alpha))^\top)$ whose parameters are $\mathbf{f}$ and the camera parameter α, where $N()$ means an operation of normalization. Then, the orthogonality between π_s and π_t can be expressed as

$$\{(\mathbf{n}_s(\mathbf{f},\alpha)\}^\top\{\mathbf{n}_t(\mathbf{f},\alpha)\} = 0. \tag{9}$$

Other types of geometrical constraints such as parallelisms can be easily formulated using the similar method.

To solve the equations described above, non-linear optimization with respect to $\mathbf{f}$ and α can be used. We implemented the numerical solver using Levenberg-Marquardt method. The determination of the initial value of $\mathbf{f}$ may be a problem. In the experiments described in this study, we construct a solution vector $\mathbf{x}_I$ from the given plane parameters and $\mathbf{f}_I = \mathbf{M}^\top\mathbf{x}_I$ is used as the initial values of $\mathbf{f}$. In this method, $\mathbf{f}_I$ is the projection of $\mathbf{x}_I$ in the space of the plane parameters whose dimension is $3N$, onto the solution space of the projective reconstruction (8) such that the metric distance between $\mathbf{f}_I$ and $\mathbf{x}_I$ is minimum. Using this process, we can obtain a set of plane parameters which fulfills the coplanarity conditions for an arbitrary set of plane parameters.

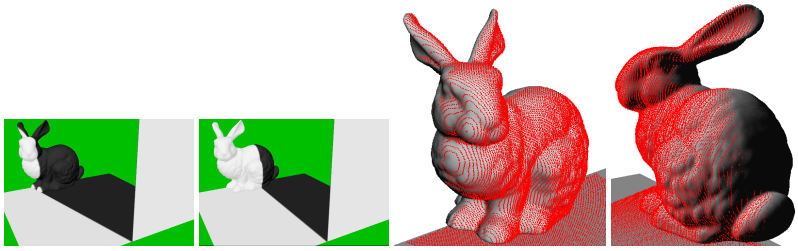

(a) (b) (c) (d)

Fig. 2. Reconstruction of simulation data:(a)(b) input images with shadows and (c)(d) reconstruction results. In the results, the shaded surfaces are ground truth and the red points are reconstructed points.

4.4 Dense reconstruction

To obtain a dense 3D shape, we also conduct a dense 3D reconstruction by using all the captured frames. The actual processes are as follows.

1. Detect the intersections between a implicit-coplanar curve on an arbitrary frame and the curves of the already estimated planes.
2. Estimate the parameters of the plane of the implicit-coplanar curve by fitting it to the known 3D points, which are retrieved from the intersections, using principal components analysis (PCA).
3. Recover all the 3D positions of the points on the implicit-coplanar curve by using the estimated plane parameters and triangulation method.
4. Iterate 1 to 3 for all frames.

5 Experiments

5.1 Simulation data(shadow of static object)

Figures 2 (a),(b) show data synthesized by CG including a square floor, a rabbit, and a perpendicular wall. 160 images were generated while moving the light source, so that the edge of the shadow scanned the rabbit. Simultaneous equations were created from intersection points between the implicit-coplanar shadow curves and lines that were drawn on the explicit planes. The initial value of nonlinear optimization was given to indicate whether the light source was located on the right or left.

By using the coplanar information, the reconstruction could be done only up to scale, so there were three DOFs remained. Since we also estimated the focal length, we needed four metric constraints. For obtaining an Euclidean solution, we used two metric constraints from the orthogonalities of the shadow planes and the floor, and other two constraints from the orthogonalities of the two corners of the floor. Figures 2 (c) and (d) show the result (red points) and the ground truth (shaded surface). We can observe the reconstruction result almost coincides with the correct shape. The RMS error (root of mean squared error) of the z-coordinates of all the reconstructed points was 2.6×10^{-3} where the average distance from the camera to the bunny was scaled to 1.0. Thus, a highly accurate reconstruction of the technique was confirmed.

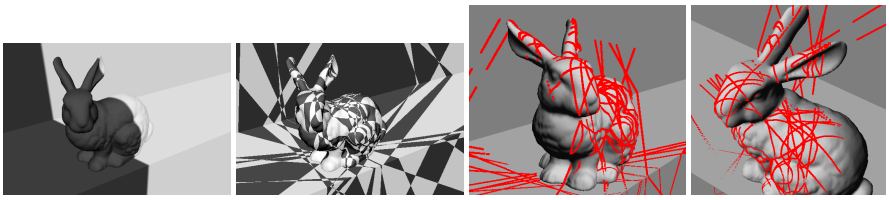

(a) (b) (c) (d)

Fig. 3. Reconstruction of simulation data (active scanning): (a) an input image, (b) explicit and implicit coplanarities, and (c)(d) reconstruction results. In the results, the shaded surfaces are ground truth and the red points are reconstructed points.

5.2 Simulation data(active scan by cast shadow)

Next, we attempted to reconstruct 3D shapes by sweeping the cast shadows on the objects by moving both a light source and a straight objects. We synthesized a sequence of images of the model of a bunny that includes 20 implicit coplanarities and three visible planes (*i.e.* explicit planes). There are three metric constraints of orthogonalities and parallelisms between the visible planes. The figure 3(a) shows an example of the synthesized images, and the figure 3(b) shows all the implicit-coplanar curves as the borders of the grid patterns. The figures 3(c) and (d) show the result. The RMS error of the z-coordinates of all the reconstructed points (normalized by the average of the z-coordinates like the previous section) was 4.6×10^{-3}. We can confirm the high accuracy of the result.

5.3 Real outdoor scene(shadow of static object)

We conducted a shape reconstruction from images acquired by outdoor fixed uncalibrated cameras. Images from the camera installed outdoors were captured periodically and a shape and the focal length of the camera was reconstructed by the proposed technique from shadows in the scene. Since the scene also contained many shadows generated by non-straight edges, the automatic extraction of complete shadows was difficult. In this experiment, these noises were eliminated by human interactions and it took about 10 minutes for the actual working time. The figure 4 (a) shows the input frame, (b) shows the detected coplanar shadow curves, (c) shows all the coplanar curves and their intersections, and (d) to (f) show the reconstruction result. The proposed technique could correctly reconstruct the scene by using images from a fixed remote camera.

5.4 Real indoor scene(active scan by cast shadow)

We conducted an indoor experiment on an actual scene by using a point light source. A video camera was directed toward a target object and multiple boxes and the scene was captured while the light source and the bar for shadowing were being moved freely. From the captured image sequence, several images were selected and the shadow curves of the bar were detected from the images. By using the detected coplanar shadow curves, we performed the 3D reconstruction up to 4 DOFs. For the metric reconstruction, orthogonalities of faces of the boxes were used. Figures 5 show the capturing scenes and the reconstruction result. In this case, since there were only small noises

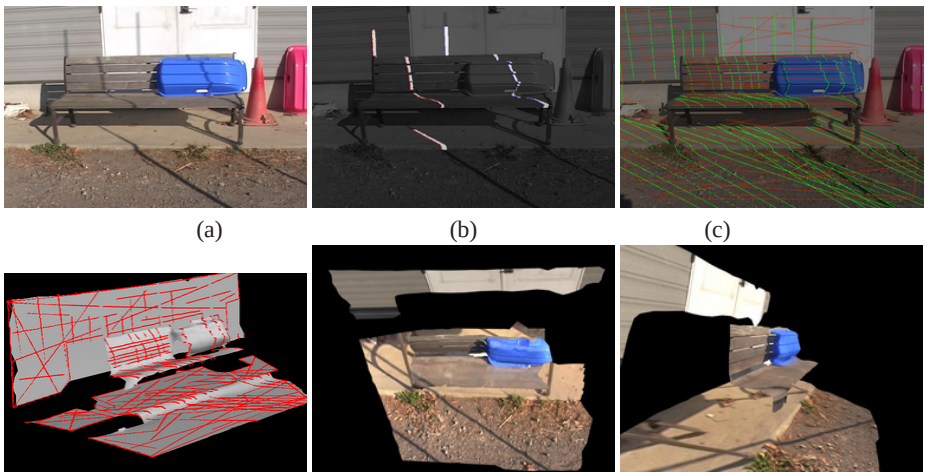

(a) (b) (c)

(d) (e) (f)

Fig. 4. Reconstruction of outdoor scene: (a) input image, (b) an example frame of the 3D segmentation result, (c) implicit (green) and explicit (red) coplanar curves, (d) reconstructed result of coplanar curves(red) and dense 3D points(shaded), and (e)(f) the textured reconstructed scene.

extracted because of indoor environment, shadow detection was stable and no human interaction was required. These results show that the dense shape is correctly reconstructed.

We also reconstructed a scene of a box (size:0.4m $\times$ 0.3m $\times$ 0.3m) and a cylinder(height:0.2m, diameter:0.2m) to evaluate accuracies of the proposed method. The process of reconstruction was conducted in the same way as the previous experiment, except that we also measured the 3D scene by an active measurement method using coded structured light [14] as the ground truth. The reconstruction result was scaled to match the ground truth using the average distance to the points. Figures 6 (a) and (b) show the capturing scene, and (c) and (d) show both the scaled reconstruction (polygon mesh) and the ground truth (red points). Although there were small differences between the reconstruction and the ground truth, the shape was correctly recovered. The RMS error of the reconstruction from the ground truth normalized by the average distance was 1.80×10^{-2}.

6 Conclusion

This paper proposed a technique capable of reconstructing a shape if only multiple shadows of straight linear objects or straight edges are available from a scene even when the light source position is unknown and the camera is not calibrated. The technique is achieved by extending the conventional method, which is used to reconstruct polyhedron from coplanar planes and its intersections, to general curved surfaces. Since reconstruction from coplanarities can be solved up to four DOFs, we proposed a technique of upgrading it to the metric solution by adding metric constraints. For the stable

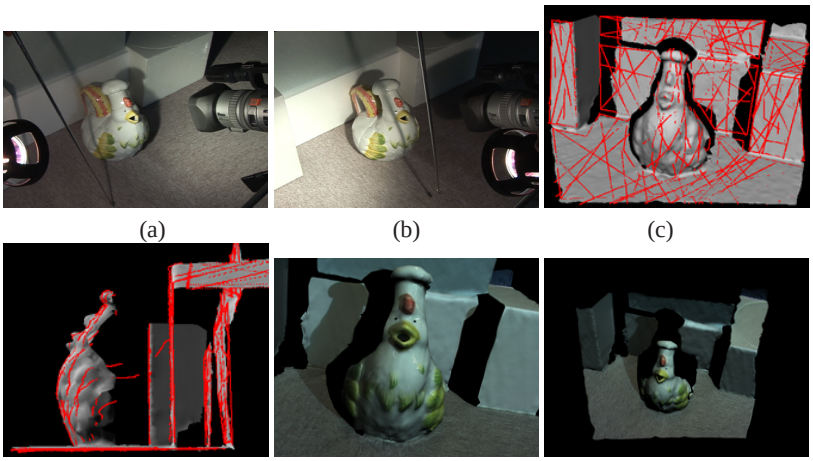

(a) (b) (c)

(d) (e) (f)

Fig. 5. Reconstruction of an indoor real scene: (a)(b) the captured frames, (c)(d) the reconstructed coplanar shadow curves (red) with dense reconstructed model(shaded), and (e)(f) the textured reconstructed model.

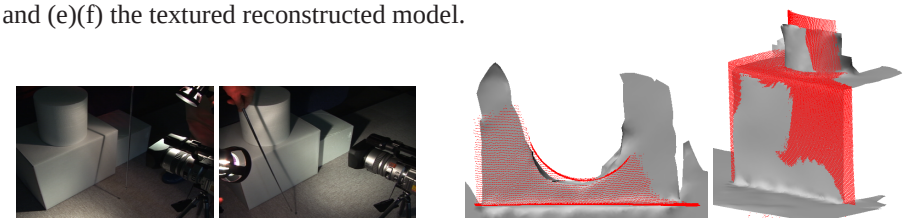

(a) (b) (c) (d)

Fig. 6. Reconstruction and evaluation of an indoor real scene: (a)(b) the captured frames and (c)(d) the reconstructed model displayed with the ground truth data (shaded model: reconstructed model, red points: ground truth).

extraction of shadow areas from a scene, we developed a spatio-temporal image processing technique. By implementing the technique and conducting an experiment using simulated and real images, accurate and dense shape reconstruction were verified.

Acknowledgement

This work was supported in part by SCOPE(Ministry of Internal Affairs and Communications, Japan).

References

1. Kriegman, D.J., Belhumeur, P.N.: What shadows reveal about object structure. Journal of the Optical Society of America **18**(8) (2001) 1804–1813 1, 2, 6
2. Bartoli, A., Sturm, P.: Constrained structure and motion from multiple uncalibrated views of a piecewise planar scene. International Journal of Computer Vision **52**(1) (2003) 45–64 2
3. Kawasaki, H., Furukawa, R.: Dense 3d reconstruction method using coplanarities and metric constraints
for line laser scanning. In: IEEE Conf. 3DIM. (2007) – 2

4. Sugihara, K.: Machine interpretation of line drawings. MIT Press, Cambridge, MA, USA (1986) 2
5. Shafer, S.A., Kanade, T.: Using shadows in finding surface orientations. Computer Vision, Graphics, and Image Processing **22**(1) (1983) 145–176 2
6. Hambrick, L.N., Loew, M.H., R. L. Carroll, J.: The entry exit method of shadow boundary segmentation. PAMI **9**(5) (1987) 597–607 2
7. Hatzitheodorou, M., Kender, J.: An optimal algorithm for the derivation of shape from shadows. In: CVPR. (1988) 486–491 2
8. Raviv, D., Pao, Y., Loparo, K.A.: Reconstruction of three-dimensional surfaces from two-dimensional binary images. IEEE Trans. on Robotics and Automation **5**(5) (1989) 701–710 2
9. Daum, M., Dudek, G.: On 3-d surface reconstruction using shape from shadows. In: CVPR. (1998) 461–468 2
10. Savarese, S., Andreetto, M., Rushmeier, H., Bernardini, F., Perona, P.: 3d reconstruction by shadow carving: Theory and practical evaluation. IJCV **71**(3) (2007) 305–336 2
11. Bouguet, J.Y., Perona, P.: 3D photography on your desk. In: ICCV. (1998) 129–149 2
12. Bouguet, J.Y., Weber, M., Perona, P.: What do planar shadows tell about scene geometry? CVPR **01** (1999) 514–520 2
13. Caspi, Y., Werman, M.: Vertical parallax from moving shadows. In: CVPR, Washington, DC, USA, IEEE Computer Society (2006) 2309–2315 2
14. Jiang, C., Ward, M.O.: Shadow segmentation and classification in a constrained environment. CVGIP: Image Underst. **59**(2) (1994) 213–225 4
15. Salvador, E., Cavallaro, A., Ebrahimi, T.: Cast shadow segmentation using invariant color features. Comput. Vis. Image Underst. **95**(2) (2004) 238–259 4
16. Sato, K., Inokuchi, S.: Range-imaging system utilizing nematic liquid crystal mask. In: Proc. of FirstICCV. (1987) 657–661 9